בס״ד

מכון ויצמן למדע
WEIZMANN INSTITUTE OF SCIENCE

Thesis for the degree
Master of Science

חבור לשם קבלת התואר
מוסמך למדעים

By
Eyal Cohen-Hoshen

מאת
אייל כהן-חושן

הגברה פלסמונית של פלואורסנציה
Plasmonic Fluorescence Enhancement

Advisor:
Prof. Israel Bar-Joseph

מנחה:
פרופ' ישראל בר-יוסף

January 14, 2009

י"ח בטבת ה'תשס"ט

Submitted to the Scientific Council of the
Weizmann Institute of Science
Rehovot, Israel

מוגש למועצה המדעית של
מכון ויצמן למדע
רחובות, ישראל

Contents

Abstract

A quantum emitter placed near the surface of a metal nanoparticle shows a tremendous increase of its emission intensity. Plasmons which are electron density fluctuations in resonance with the illuminating electromagnetic field, cause an enhancement of the electromagnetic field at short distances from the metal nano particle surface. There are three major mechanisms involved in this effect. The first is due to the enhanced electromagnetic field which causes an increased absorption by the quantum emitter. The second enhancement mechanism is a reduction in the excited state lifetime of the quantum emitter due to this strong field. The third effect is an inhibition rather than enhancement of the emission by an energy transfer mechanism from the quantum emitter to the metal nanoparticle. All of these effects are inherently distance dependent on a short scale of a few nanometers. Some of these effects were measured for molecules as well as in chemically grown quantum dots adsorbed on rough metallic surfaces and on metal nanoparticles. The measured enhancement factors are between 2-20 fold, and are much less than theoretical predictions of up to 100. The aim of this work is a detailed study of these effects on the single object level in a way that would take the enhancement to its maximum. For achieving this goal we employ novel methods of nano-fabrication and use a state of the art fluorescence measurement system with single molecule detection capabilities.

Chapter 1

Introduction

1.1 Overview - Plasmonics

After a hundred years of being left over, the wonders of interaction of light with noble metal particles are rising again in the fields of science. Faraday [1] was fascinated with the strong red color of colloidal gold solutions and conducted experiments on their optical properties. Theoretical explanation of this strong scattering was given by Mie in 1908 in his work on the scattering of light by gold colloids. His phenomenological explanation of the strong absorbance and scattering was later understood to be related with excitation of plasmon resonances inside the metal nanoparticles (MNPs) [2]. Plasmons are excitations of electron density fluctuations in resonance with the illuminating electromagnetic field. But why is there such a revival to this field nowadays? Well, the presence of plasmons in the MNP induces a strong electromagnetic field near its surface on the scale of a few nanometers, which is the key for many new interesting phenomena and applications. Nowadays with the emergence of nanotechnology and the capabilities of electron microscopy, single molecule detection, and sophisticated chemical synthesis, there is an ability to measure these short range interactions and to use them for realizing new applications. Short distance near field interactions between illuminated MNPs are realized in experiments like the focusing and guiding of light in sub-diffraction limit areas[3, 4]. MNPs short range interaction is evident in their far field extinction measurements. Surface Enhanced Raman Scattering (SERS) from molecules absorbed

on silver MNP aggregates was found to be enhanced by as much as 15 orders of magnitude comparing to regular Raman scattering. Fluorescence near MNPs seems to be enhanced by up to an order of magnitude. These novel experiments together with better theoretical understanding and modeling, are lying the seeds for a whole variety of new devices and applications. The focusing and propagation of light in nanoscale distances could be used in the field of photonics and electro-optics for developing sub-diffraction limit wave guides and optical inter-connects. SERS and Plasmonic Enhanced Fluorescence could be used in detection of single molecules, which is important for basic research as well as for applications in medicine and biology. Plasmon short range interactions could be also used in biology for detecting short distances between interacting biomolecules[5]. These plasmonic effects could be of use in improving photovoltaic cells, tera-hertz electronics and cavity QED experiments related to basic QM manipulations and quantum computing. These phenomena are considered now to be a part of a new field called *Plasmonics*.

1.2 Scientific Background

Plasmonic Fluorescence Enhancement is one interesting phenomenon in the emerging field of plasmonics. An illuminated quantum emitter (QE) placed at a short distance from a MNP surface shows an increase of its emission intensity. Experiments measuring this effect show a 2-20 fold enhancement of fluorescence [9, 10] depending on the metal fluorophor system. On the other hand, at short distances there is a partial or total quenching of the emission intensity. Previous work on this subject began at the eighties [6] on organic fluorophors adsorbed on metal surfaces. There are several studies that measure the distance dependence of this effect indicatibg that there is an optimal distance for the enhancement, but it changes from one system to another[10, 11]. Another important observation is related to the effect of the interaction between MNP and QE on the radiative lifetime. Time domain measurements [7] show that the excited state lifetime is shortened by up to 1000 fold in a system of QDs near a gold roughened surface. I will now review a theoretical model that is able to put all three aspects of absorption enhancement, quenching and reduction in radiative lifetime in one framework. This would be a sufficient framework for our research purposes.

1.2.1 Theoretical Framework

There are three distinct mechanisms that are involved in plasmonic emission of a QE near a MNP. Two of them are enhancement mechanisms and the third is a quenching mechanism.

The first enhancement mechanism is a *reduction of the lifetime of the excited state* that results in an increase in the number of emitted photons per unit time. This is explained by semi-classical models [8, 12] of a radiating dipole near a MNP surface, or by a quantum mechanical model which relies on the Purcell effect [13]. This mechanism requires a spectral overlap between the plasmon resonance and the QE *emission* energy.

The second enhancement mechanism is due to *enhanced absorption*. The strong field near the MNP surface implies that more photons are absorbed by the QE per unit time. This effect depends on the spectral overlap between plasmon resonance energy and the QE *absorption* band.

However, the presence of the MNP introduce also a *non-radiative loss channel* in the form of a non-radiative energy transfer from the QE to the MNP. Upon excitation, the QE acquires a transition dipole. This dipole interacts with the MNP by a coulomb interaction and the energy is transferred to the MNP in the form of an excitation of a non-radiative plasmon.

1.2.1.1 The Emission Enhancement Model

The efficiency of the enhancement depends on the interplay between the enhancement mechanisms and the loss channels. These mechanisms depend on distance in different ways, yet all are decaying on the nanometer scale. I will use a model given in the work of A. Govorov, G. Bryant, et al. [14] to explain the interplay between these effects.

This work introduces a rate equation for the population of excitons in a QD. It is solved for a steady state illumination and gives the emission intensity. The radiative and non-radiative decay rates of the QD are given as inputs to this model. The plasmon resonance enters the model in the form of frequency dependent enhancement factor of the electromagnetic field intensity. The physical properties of the materials of the MNP, QD and the environment, enter the model in the form of frequency dependent dielectric functions.

The rate of change in the number of excitons,n, in the QD is given by

$$\frac{dn}{dt} = -\gamma_{tot} \cdot n + I_{abs} \tag{1.1}$$

where I_{abs} is the intensity of light absorption in the QD. The exciton recombination rate, γ_{tot}, includes several mechanisms of recombination

$$\gamma_{tot} = \gamma_r + \gamma_{nr}^0 + \gamma_{nrm} \tag{1.2}$$

where γ_r and γ_{nr}^0 are the radiative and non-radiative rates of the exciton in the QD. The regular non-radiative rate is assumed not to change in the presence of the MNP. γ_{nrm} is the exciton recombination rate of the QD due to energy transfer to the MNP in the form of a non-radiative plasmon excitation. Under a constant illumination the steady state solution for Eq. (1.1) is $n = \frac{I_{abs}}{\gamma_{tot}}$, hence the quantum yield of the QD is given by

$$Y = \frac{\#\ of\ radiatied\ photons}{\#\ of\ incoming\ photons} = \frac{\gamma_r n}{I_{abs}} = \frac{\gamma_r}{\gamma_{tot}} \tag{1.3}$$

in the presence of the MNP. This is to be compared to the bare quantum yield $Y^0 = \frac{\gamma_r^0}{\gamma_{tot}^0}$. The intensity enhancement factor, $P(\omega)$ (Eq. 1.4), is given by the ratio between the enhanced electric field squared, in the presence of the MNP, and the electric field squared of the illuminating field. These fields are averaged over time,volume of the QD and the angle in the plane perpendicular to the MNP-QD axis (t, V_{QD} and ϕ, respectively). The enhancement factor depends on the distance from the MNP center, d, and on θ, the angle between the MNP-QD axis and the illuminating field.

$$P(\omega, d, \theta) = \frac{\left\langle |\overrightarrow{E}_{enh}(\omega, t, d, \theta, \phi)|^2 \right\rangle_{\phi,t,V_{QD}}}{\left\langle |\overrightarrow{E}|^2 \right\rangle_{t,V_{QD}}} \tag{1.4}$$

Taking this factor at the illuminating laser frequency, ω_l, gives an enhanced absorption term

$$I_{abs} = P(\omega_l, R) \cdot I_{abs}^0, \tag{1.5}$$

while taking this factor at the frequency of the QD emission, ω_e, gives a modified radiative lifetime

$$\gamma_r = P(\omega_e) \cdot \gamma_r^0. \tag{1.6}$$

The total emission intensity, I_e, is given by substituting Eq. (1.6) and Eq. (1.5) into

$$I_e(\omega_e) = \frac{\gamma_r \cdot I_{abs}}{\gamma_r + \gamma_{nr}^0 + \gamma_{nrm}(\omega_e)} \tag{1.7}$$

to give

$$I_e(\omega_e) = \frac{[P(\omega_e, d, \theta) \cdot \gamma_r^0] \cdot [P(\omega_l, d, \theta) \cdot I_{abs}^0]}{[P(\omega_e, d, \theta) \cdot \gamma_r^0] + \gamma_{nr}^0 + \gamma_{nrm}(\omega_e)} \tag{1.8}$$

The justification for the modification of the radiative lifetime could be found elsewhere [8, 12, 13]. In this work I wish to focus on the mechanism of absorption enhancement and wish to separate it from the effect of the modified radiative decay rate. I would do this by choosing a MNP system that would not yield a significant electric field enhancement at the energies where the QD emits. In this way the radiative decay rate would not be significantly modified. Under this assumption Eq. (1.7) reduces to

$$I_e(\omega_e) \quad = \quad \frac{\gamma_r^0 \cdot [P(\omega_l, d, \theta) \cdot I_{abs}^0]}{\gamma_r^0 + \gamma_{nr}^0 + \gamma_{nrm}(\omega_e)} \tag{1.9}$$

so we are left only with the interplay between the *enhancement of the absorption* in $P(\omega_l, d, \theta)$ and the *additional loss channel* that comes in $\gamma_{nrm}(\omega_e)$.

1.2.1.2 The Field Enhancement Factor $P(\omega, d)$

As formulated in the previous section, both the enhancement of the absorption and the reduction of the excited state lifetime depend on the local enhancement of the electromagnetic field intensity, $P(\omega, d)$ as in Eq. (1.4). The electromagnetic field could be calculated analytically from the Maxwell's equations as was done by Mie in 1908 [15] or by numerical methods like the finite-difference time-domain method (FDTD)[9]. For our purposes we could use a simpler treatment under some assumptions.

The R $<<\lambda$ Limit and The Quasi-static Approximation. In our simple treatment we make two approximations. In the case of a MNP with a radius $R << \lambda$ (the wavelength of the illuminating electromagnetic field) we can assume that the whole particle is under the influence of a

constant electromagnetic field. The second approximation we make is the Quasi-static approximation. It suggests that the metal responds immediately to the electromagnetic field, hence, we could solve the electrostatic problem of a dielectric sphere placed in a uniform constant electromagnetic field in a dielectric medium. It is surprising that we can get much of the observed phenomena by this simple model.

I will follow a derivation given in the books of U. Kreibig and S. Maier [18, 19]. This derivation starts with the Laplace equation $\nabla^2\phi_{out} = 0$ outside the MNP, with sharp boundary conditions at the sphere surface. The solution for ϕ_{out} is

$$\phi_{out} = -E_0 r cos\theta + \frac{\epsilon - \epsilon_m}{\epsilon + 2\epsilon_m} E_0 a^3 \frac{cos\theta}{r^2}. \tag{1.10}$$

The first term is the contribution of the external field and the second term could be rewritten in the form of a potential induced by a dipole $\overrightarrow{P}$ sitting at the origin.

$$\phi_{out} = -E_0 r cos\theta + \frac{\overrightarrow{P} \cdot \overrightarrow{r}}{4\pi\epsilon_0\epsilon_m r^3} \tag{1.11}$$

The electric field is given by $\overrightarrow{E}_{out} = -\overrightarrow{\nabla}\phi_{out}$.

$$\overrightarrow{E}_{out} = \overrightarrow{E}_0 + \frac{3\overrightarrow{n}(\overrightarrow{n} \cdot \overrightarrow{p} - \overrightarrow{p})}{4\pi\epsilon_0\epsilon_m} \frac{1}{r^3} \tag{1.12}$$

Where the dipole is given by

$$\overrightarrow{P} = 4\pi\epsilon_0\epsilon_m a^3 \frac{\epsilon - \epsilon_m}{\epsilon + \epsilon_m} \overrightarrow{E}_0 \tag{1.13}$$

We see that the applied field induces a dipole moment inside the sphere of a magnitude proportional to that of $\overrightarrow{E_0}$. In order to get the solution for a time varying field, under the quasi-static approximations we just have to substitute a time varying field $\overrightarrow{E}(\omega, t)$ inside the static solution, and $\epsilon(\omega)$ instead of ϵ .

This simple model already gives some of the size dependence and the frequency dependence of the resonance. The magnitude of the resonance is proportional to the volume of the sphere given by the a^3 factor in Eq. (1.13). The frequency dependence and also the magnitude is given by the resonance condition for the dipole:

$$|\epsilon + 2\epsilon_m| = Minimum, \tag{1.14}$$

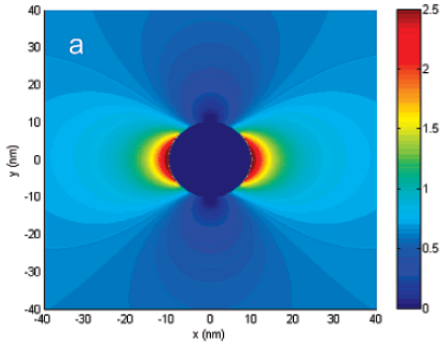

Figure 1.1: The electric field near an illuminated silver MNP (FDTD calculation)[9].

and for a complex function $\epsilon = \epsilon_1 + i\epsilon_2$ this would be

$$[\epsilon(\omega) + 2\epsilon_m]^2 + [\epsilon_2(\omega)]^2 = Minimum. \tag{1.15}$$

The dependence of the resonance on the medium, comes into play through the dielectric function of the medium, ϵ_m. It is assumed to be constant in the visible light frequencies which is true in the case of water. The dependence of the resonance on the frequency is given by the frequency dependence of the dielectric response of the metal. In order to get a sharp resonance at a certain frequency there are two demands. The first is that the real part of ϵ should be close in magnitude to $2\epsilon_m$, yet with an opposite sign. The second demand is that the imaginary part, ϵ_2, would be sufficiently low at that frequency. The solution also gives the spatial dependence of the electromagnetic field, $\frac{1}{r^3}$. These features could be seen by substituting Eq. (1.13) into Eq. (1.12). An illustration of the spatial dependence of the electric field is given in Figure 1.1. Taking the electric field obtained by this calculation and substituting it in Eq. (1.4) from the previous section gives the desired intensity enhancement factor $P(\omega, d, \theta)$.

Although this model correctly predicts that the intensity of the resonance scales like the volume of the MNP, it still lacks an explanation for the redshift of the resonance for larger particle. The reason for this is that the assumption of $R << \lambda$ stops to be accurate at this range. For large particles the electromagnetic field could not be taken as a constant as it would be retarded, or vary spatially over the particle volume. In order to explain this, a full theory was given in 1908 by G. Mie.[15] who analytically solved the exact electrodynamic problem of a dielectric sphere in

an external field. He solved the Maxwell's equations using a multiple expansion of the incoming electromagnetic field in spherical coordinates. This solution was better organized and reduce by Born [17] in is famous book in optics, and by Stratton in his book on electromagnetic theory [16].

1.2.1.3 The Non-Radiative Energy Transfer Rate, $\gamma_{nrm}(\omega_e)$.

Non radiative energy transfer has to do with the decay of an exciton into an excitation of a non-radiative plasmon in the MNP. This is due to coulomb interaction between the charge distributions inside the QD and inside the MNP. A simple case would be to take both the QD and the MNP as point dipoles and to apply the famous Forster Resonance Energy Transfer (FRET) mechanism which gives $\gamma_{nrm} \propto \frac{1}{r^6}$ [20]. I chose not to give here a full explanation of this because the problem of the QD near a MNP sphere at such short distances could not be treated as a point interactions. A full treatment of a coulomb interaction between a hole and an electron in the semiconducting QD and the whole dielectric response of the metal sphere should be taken into account. Such a treatment is given to the problem by Garnet and Govorov. Their calculation gives a $\gamma_{nrm} \propto \frac{1}{r^4}$ dependence at short distances while at larger distances it gives the regular $\frac{1}{r^6}$ as in the Forster model .

1.2.1.4 The Dielectric Function of MNPs.

The dielectric function of MNPs manifests their plasmon resonance behavior as seen in Eq. (1.15). I will now discuss the factors that govern the spectral dependence of the dielectric function.

$$\epsilon(\omega) = \epsilon_1 + i\epsilon_2 = 1 - \frac{\omega_p^2}{\omega^2} + \chi_{core} + i(1 - \frac{\omega_p^2}{\omega^3}\Gamma + \chi_{interband}) \tag{1.16}$$

Some of the factors in $\epsilon(\omega)$ are universal, while other factors change from one metal to another. The intrinsic factors that change from metal to metal are the dielectric response due to inter-band transitions, $\chi_{interband}$, and the response due to the polarizability of the core electrons, χ_{core}. The resonance energy depends on the spectral dependence of the core polarization and the spectral position of the inter-band transition with respect to the plasmon resonance energy. The universal factors resemble the free electron behavior of metals. They include the size and boundary features of the MNP, which affect the plasmon behavior.

Eq. (1.16) shows the characteristic behavior of a bulk metal. The size and shape dependence would enter the equation by introducing a size dependent damping factor, $\Gamma(R)$, and also a modification for the real part of the function. The reason for the size dependence arises from the fact that for small enough particles the mean free path of the electrons becomes comparable or even larger than the MNP size. In this case, electrons would have an absolutely free motion inside the MNP and would scatter only from the boundaries of the particle. This behavior depends on the size and shape of the particles.

These contributions of the free electron behavior, χ_{core} and $\chi_{interband}$ give us an understanding of the difference between the optical responses of different metals. I will concentrate on the difference between Au and Ag. Au plasmon resonance is strongly affected by the inter-band transition which gives rise to a larger imaginary part ϵ_2 at the inter-band frequency regime. The minimum of ϵ_2 in the case of gold is therefore redshifted, giving a plasmon resonance at 520 nm. However, for silver ϵ_2 drops at around 300 nm because the inter-band transition appears at higher energies. The contributions of core polarization and the free electron behavior give a resonance at around 400 nm. The reader is referred to a thorough treatment of the dielectric function and plasmons in metals in the book of U. Kreibig [18] and by David Pines in his book on elementary excitations in solids [21].

For practical needs, the dielectric function could be derived from experimental results of optical measurements. Such an approach is used by Kreibig [22] to get the exact dielectric function of the MNPs with the use of measured extinction spectra which is the most simple experiment one can do. Kreibig measures the extinction spectrum of MNPs in the visible frequencies and by extrapolation with measurements of others he gets the extinction for the whole spectrum. By using a Kramers-Kronig analysis he gets the complimentary real function of the *Relative Dispersion* which cannot be measured for these small particles. By using Gans-Happel theory [22] he gets the exact dielectric imaginary and real functions.

1.3 The Research Goals

I would like to conduct an experiment that will take fluorescence enhancement measurements to its 100 fold theoretical limit. For doing that I would have to make *single object measurements* and to make a system that would have a minimal *non-radiative energy transfer*.

Conducting a study on the *single object* level would give an answer for the faults of ensemble measurements. Ensemble measurements have three major drawbacks. The first is a varying number of fluorophors on each MNP. The second is that instead of a defined polarization there would be a whole distribution of relative polarizations between the laser and the MNP-QE axis. The third is that instead of a defined distance there is a whole distribution of MNP-QE distances. As a consequence, the measurement would be an average over the distance and polarization distributions and since the interaction strongly depend on the orientation and the distance between the MNP and the QD the measured enhancement would be significantly reduced.

I shall use chemically synthesized semiconductor QDs as my QEs since they have several convenient features. First of all, the use of QDs is preferable over organic fluorophors as they could be tailored to emit light at any desired color and they show much less photo-bleaching. But the main advantage of QDs in this experiment is that unlike organic fluorophors, QDs can be identified easily on the single object level in both transmission and scanning electron microscopes. By using smart synthetic routes, a controlled synthesis and 100% verification of single MNP single QD conjugate production is available. This system enables a detailed study of the dependence of emission enhancement on the distance as well as on polarization.

The way to control the *non-radiative energy transfer rate* rely on the understanding we have of the enhancement mechanisms. The two enhancement mechanisms arise from the spectral overlap of the plasmon resonance and the QE absorption band or emission band. I would choose a MNP-QD system that have a good overlap between the MNP plasmon resonance and the QD absorption band rather than an overlap with its emission band. The use of QDs offers an additional advantage that would give an answer to this problem. QDs emission is strongly redshifted relative to their absorption. This separation would make the non radiative energy transfer less probable because we can take a MNP-QD system where the emission spectrum does not overlap the plasmon resonance

energy.

The outline for this work: This work begins with a detailed description of the experimental methods in Chapter 2. Chapter 3 starts with a discussion on the implications of our current understanding of the enhancement mechanisms on choosing a MNP-QD system in section 3.1. Sections 3.2 and 3.3 present the experimental results of the synthesis and fluorescence measurements, respectively, and Chapter 4 ends this work with concluding remarks and plans for the future .

Chapter 2

Experimental Methods

Taking the considerations in the previous section in mind I shall review the methods that are used in this work. These methods would allow the realization of fluorescence enhancement on the single object level. It begins with a controlled synthesis of MNPs with the desired size which is responsible for the plasmon resonance intensity and energy. After that I will discuss the issue of colloidal stability. The possibility to make single particle conjugates relies on the ability of stabilizing the particle dispersions against aggregation. After that I shall present a few methods used in preparing MNP-QD conjugates with a defined separation. The methods used for measuring fluorescence are standard and are described in appendix A.

2.1 The Synthesis of Colloidal MNPs

Plasmon resonance in MNPs strongly depends on their size and shape. A good control over the size distribution and shape of the particles is therefore needed in order to match the resonance energy with the available laser energy. How could we control the size distribution of the particles in the synthesis? For answering this question a good understanding on the mechanism of growth of the particles is needed.

The first scientific studies of colloidal metal dispersions were established in 1857 by Michael Faraday[1]. He developed new preparative methods for colloidal gold. The most popular method to date is Turkevich's modification to Hauser and Lynn's citrate reduction route [23, 24]. The

procedure involves the reduction of metal cations into metal atoms by a reducing agent . Upon over-saturation of the solution metal clusters start to nucleate. For a spherical cluster that liberates -Gv Joules per cubic centimeter during formation (here Gv is a negative quantity), but which must pay the positive cost of σ Joules per square centimeter of surface interfacing with the world around, the free energy needed to form a cluster of radius r is $W = \frac{4}{3}\pi r^3 G_v + 4\pi r^2 \sigma$. It costs free energy to add atoms to this cluster until the radius reaches $r^* = -\frac{2\sigma}{G_v}$ where $\frac{dW}{dr} = 0$. As the process of formation of new metal nuclei cost more energy than the adsorption of metal atoms on the surface of a cluster larger than r^*, the latter would be favorable kinetically. Hence, metal clusters would start to grow at the expense of forming new nuclei in the dispersion. The products of such a reaction yield a dispersion of particles with a wide size distribution, because nucleation and growth could occur at the same time, hence, particle created at a later time would have a smaller final size.

The preparation of size homo-dispersed metal clusters solution could be achieved by "seeded growth" techniques, which were first described in 1906 by Zsigmondy [25]. The principle is to control the reaction conditions in such a way that nucleation of new seeds and the further growth of these seeds into large particles would be timely separated. This could be achieved in two ways. One way is to add, formerly grown, nuclei to the precursor solution so growth would be much favorable over nucleation. Another way is to add a surfactant to the solution that would cause a very rapid nucleation step by lowering σ.

Another effect that causes the narrowing of the size distribution of particles arises from the fact that the growth rate is a decreasing function of the diameter of the particles. The particle diameter grows by constant steps of the metal atom diameter, but the surface coverage increase with the increasing diameter of the particle, hence, as the particle grows it would take more time to cover its surface with metal atoms. This fact would cause the size distribution to "focus" as the particles grow large.

2.2 Colloidal Stability

Due to the presence of attraction forces, particles in a dispersion aggregate to form bulk solid. It would not be possible to measure fluorescence of single objects without first having a stable dispersion with no significant aggregation. But how could this be done? First of all let's discuss the parameters influencing this stability and then maybe we could find a way to control them.

A charged surface put in an ionic solution is said to form an Electrical Double Layer of ions surrounding it. The first layer (Stern) is of dense oppositely charged ions and the second layer is a diffuse layer (Gouy) of ions with the same charge. (Fig. 2.1)

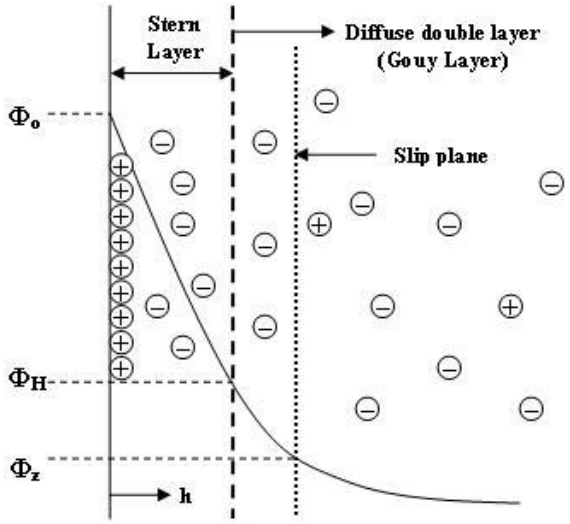

Figure 2.1: The electrical double layer potential.

The diffuse layer can move under tangential stress. There is a conventionally introduced plane in the diffuse layer, called the slipping plain, that separates the mobile fluid from the fluid that remains attached to the surface. It is useful to define a quantity which is called ζ as the difference between the potential at the slipping plane and the potential at the bulk solution. ζ is a measure for the electric charge at the surface of the particle. It is directly connected to the electrokinetic radius of the particle, the distance from the particle surface and the slipping, a useful quantity in electrophoresis. A formulation of the interactions of charged spheres in an electrolytic solution in the form of distance dependent energy potentials was done by Derajuin, Landau, Verwey, and

Overbeek in the 1940s and is called the DLVO theory[26]:

$$U(r) = kT\zeta^2\lambda_B \left(\frac{\exp(\kappa a)}{1+\kappa a}\right)^2 \exp^{-\kappa r} \; - \; \frac{A}{12\pi} r^{-2} \tag{2.1}$$

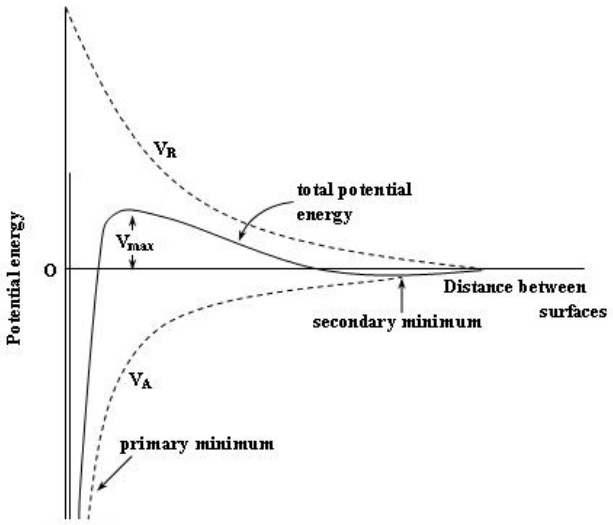

Figure 2.2: The DLVO potential.

The interaction involves an attraction term which is the Van Der Waals attraction potential which goes like $-\frac{1}{r^2}$ and depends on the type of material by the Hammaker constant A. The Hammaker constant of silver is much larger than that of gold, and this is the main reason why stable silver colloid dispersion are hard to synthesize. The repulsion term is not just a Coulomb term but has the behavior of a Yukawa potential, which is present because of the screening of the charged surfaces of the particles by the electrolytic solution. The parameterκ^{-1} is the Debye screening length of a point charge in electrolytic environment, and is inversely proportional to the concentration of the ions in the solution. A schematic description of the DLVO potential is shown in Fig. 2.2.

Stabilizing the MNP dispersion against the formation of aggregates is crucial for MNP conjugates on the single object level. The control of the parameters like the ionic concentration of the solution and the surface charge of the particles gives the ability to stabilize the dispersion against aggregation. In section 3.2.1.2 I will show the specific stabilization methods used in this study.

2.3 MNP-QD Conjugates

After having a stable silver MNP dispersion we would like to form MNP-QD conjugates with a well defined separation. But how could such a delicate control over the distance between them could be maintained? Well, it could be done by cross-linking them with a molecule or a polymer of a well defined length. Caution should be taken, the spacer should be transparent to the light at all the energies between the absorbance energy and the emission energy, otherwise it would influence the emission process. In this work I have chosen a few ways to achieve that, and they will be reviewed in this section.

2.3.1 MNPs and QDs Monolayers Separated by Polymers.

The most simple method to control the distance between the QD to the MNP is by adsorbing the QDs on a substrate then apply a transparent layer with a desired thickness on-top(could be of any material that is transparent to the appropriate frequencies). Finally on top of that, to adsorb a layer of MNPs. But how can this adsorbance be of a controlled nature and yield a homogeneous surface density of particles? This could not be done relying only on the accidental adsorbance due to van der Waals interaction.

The technique used in this work is known as Layer by Layer (LBL) coating [27, 29]. The idea was first introduced by Irving Langmuir, who suggested that ions will form a mono-layer upon adsorption on a charged surface [31]. After adsorption of the first layer, ions of the same kind would not be further adsorbed to form a second layer because of electrostatic repulsion from the first layer. Subsequent layers of opposite charges could be adsorbed in the same manner and form a thin film. This method has the spatial resolution of the single ion's diameter. Using his technique with Poly-electrolytes, which are polymers of ionic nature, would give two extra benefits. The first is that the layer would be more stable against thermal fluctuations, and the second is that each layer would not have to be of thickness of the single ion, but could be as thick as the polymer mean thickness which is about 0.5 nm in our case. An illustration of this method is given in Fig. 2.3.

I will use this method in creating devices with a MNP monolayer and a QD monolayer separated

by a few polyelectrolyte layers.

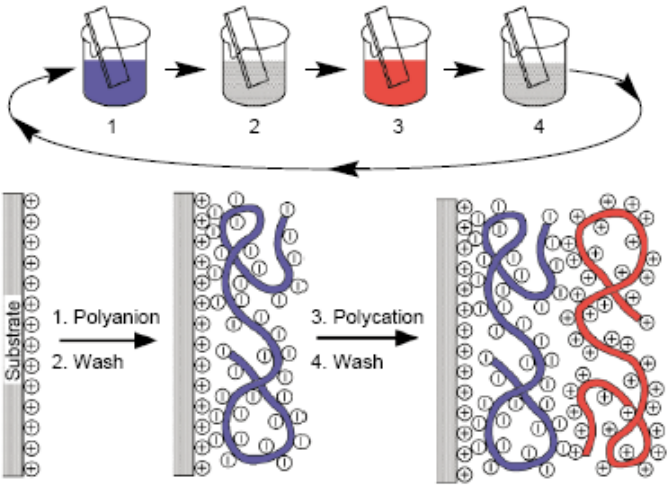

Figure 2.3: Preparation of poly-electrolyte thin films [32].

2.3.2 MNP - Polymer - QD Conjugates

How could one form specific conjugation of two different species in a solution? How could a well defined separation be maintained? One way for doing that uses a modification of the layer by layer assembly method for coating small particles.

Caruso et. al used the method of LBL coating to coat single particles by subsequent adsorption of poly-electrolyte layers. This gives us the ability to make conjugate at the single particle level and control the distance by the number of polymer layers. In his work he coated gold colloids of 7 nm and 30 nm[30].

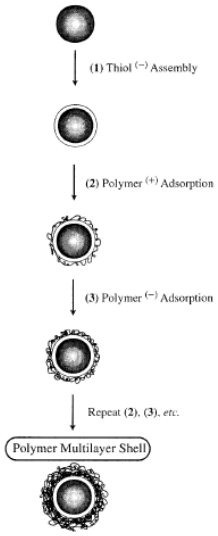

Figure 2.4: Poly-electrolyte coating of a single MNP [30].

In another work he managed to coat $1\mu m$ polystyrene spheres and adsorb on them small spheres as shown in Fig. 2.5.

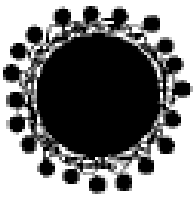

Figure 2.5: An illustration of a PS sphere coated with smaller nanoparticles[33].

In a similar manner as the above method for slide coverage, also here after the last step of polymer coating with a positively charged PDADAMC a layer of negatively charged QDs was absorbed. Single particle conjugates could be achieved by controlling the concentration ratio between MNP and QD dispersions.

2.3.3 DNA Conjugates

A novel method of specific conjugation of particles was beautifully demonstrated by the Alivisatos group [34, 35]. This method relies on the ability to synthesize oligo(short)-DNA strands with a

tail that could be modified for conjugation. In their work they have demonstrated the binding of thiol modified DNA of length varying from 30-90 bases, to gold MNP of sizes up to 20 nm. They have demonstrated the isolation of MNPs conjugated to a defined number of DNA strands by the means of gel electrophoresis (Fig. 2.6) as well as HPLC.

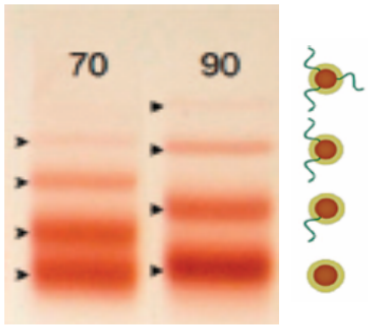

Figure 2.6: Agarose gel electrophoresis separation of MNP with discrete number of DNAs [34].

This method gives them the ability to make MNP - MNP conjugates of various kinds by using the specific interaction between complimentary DNA strands. This is demonstrated in figures from their article (Fig. 2.7) which show their ability to make nanostructures on demand. A large particle with a few DNA strands conjugated to small particles with 1 strand each gives a complex structure.

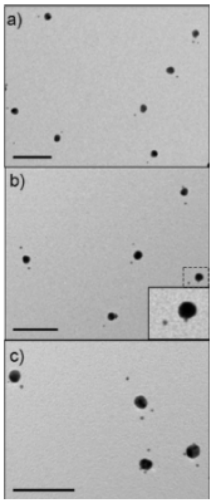

Figure 2.7: Complex gold MNP structures by DNA conjugation [34].

Chapter 3

Experimental Results

3.1 Experimental Considerations - Choosing The Right MNP-QD System.

The goal of our study is to take fluorescence enhancement to its edge. We want to conduct measurements on single MNP-QD conjugates with a well defined separation and orientation, while reducing the non radiative energy transfer loss channel. In this section I will discuss the considerations needed in order to achieve this goal. The proper choice of the QDs, the right metal and size of the MNPs will lead to the desired separation of the emission enhancement effect from the effect of absorption enhancement.

3.1.1 Quantum Dots

Semiconductor Quantum Dots absorbs above their band gap and as the energy is higher more states are available for absorbance, so the cross-section is larger. Emission though, occurs only at the band edge. Excitons with higher energies quickly relax to the band edge via phonon assisted processes with a time scale of a few picoseconds, much shorter than the typical lifetime, which is about 200 nanoseconds [7]. The absorbance and emission spectra are shown in Fig. 3.1.

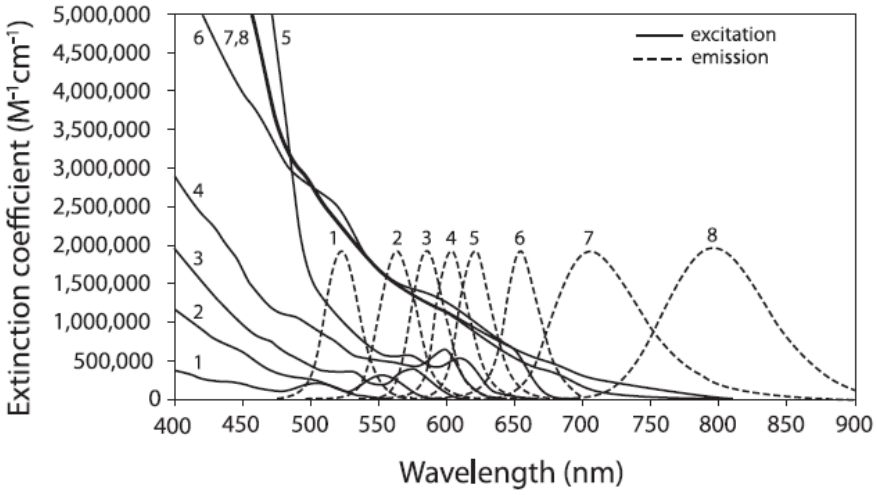

Figure 3.1: Absorption and emission spectrum of QD [Invitrogen].

In this experiment I am not interested in coupling the MNP plasmon resonance to the emission energy of the QD, but rather to the absorption. Hence, in order to have a large fluorescence signal I would choose QDs with the largest absorption cross section in the relevant energy range of the MNP plasmon resonance. This consideration would lead to selecting be red emitting QDs with a large diameter. We have decided to work with CdSe/ZnS QD with a mean diameter of 7nm with emission at 600 nm. This is one of the largest CdSe/ZnS QDs available so it could be easily detected in TEM or SEM.

3.1.2 MNPs - Metal and Size Choice.

What metal should we choose? QD absorbance cross-section is increasing with the energy (Fig. 3.1) , hence, the best absorption enhancement would be at the blue side of the spectrum. The plasmon resonance of gold MNPs are around 520 nm while for silver it is around 400 nm. Therefore for absorption enhancement, silver MNPs would be more suitable. An additional advantage of silver over gold is that silver has a much more intense plasmon resonance due to a weaker coupling of silver inter-band transition and the plasmon resonance energy as discussed in section 1.2[18].

What size of silver MNP is best suitable for this measurement? The plasmon resonance energy

and the intensity vary with the size of the MNP (Fig. 3.2). Hence, one can fine tune the plasmon by controlling the MNP size. On one hand the field enhancement intensity is an increasing function of the MNP size. On the other hand though, the resonance energy is a decreasing function of the MNP size. Thus, large MNPs would have a more intense plasmon resonance but at an energy that would couple less efficiently to the QD absorption. An optimization has to be made in choosing the best size to give the most intense plasmon resonance with the best overlap with the QD absorption. Another important factor is the overlap of the plasmon resonance energy and the energy of the laser available for measurements. It is hard to tell in advance what size of particles would give the best enhancement. In this work I use 30 nm and 60 nm MNPs that have a plasmon resonance at the energy of two available laser systems. 30 nm MNP have a plasmon resonance at 402 nm in aqueous dispersion and are excited by a 405 nm line given by a diode laser. The 60 nm MNPs have a plasmon resonance at 458 nm and are used with the 458 nm line of an Argon laser.

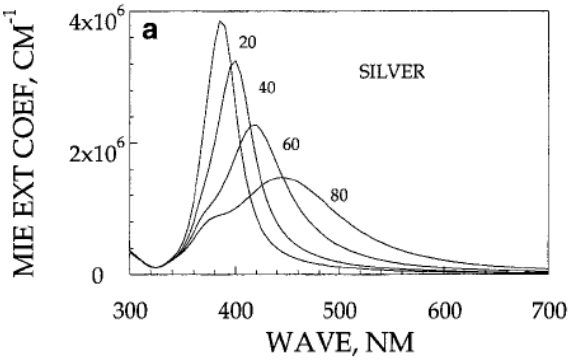

Figure 3.2: Silver MNP extinction coefficients. The numbers near each graph is the particle diameter in nm [36]. The extinction coefficient is the extinction cross-section normalized by the physical cross-section of the particle. It seems to be a decreasing function of the particle size. However, the enhancement of the field intensity depends on the extinction cross-section and not on the normalized extinction coefficient and therefore increases with the particle size.

3.2 Synthesis and Fabrication

The purpose of this work is to study fluorescence enhancement at the single object level. The main problem of such a task is producing well defined MNP-QD conjugates. I started this work with a simple method of adsorbing MNP and QD monolayers on a surface with a number of polymer layers separation. The second method I use is LBL coating of silver MNPs and then adsorbing QDs on the last layer. This method did not give the desired result of single object measurement and was used only in ensembe measurement because the MNPs did not have on them a well defined number of QDs but rather a distribution of the number of QDs. Another method that should give a more specific binding is the use of DNA in conjugating MNPs and QDs.

3.2.1 Silver MNPs

3.2.1.1 Synthesis

Various methods for metal cluster synthesis are available in the literature. The most known procedure for silver particle growth was published by Lee and Meisel [37] in 1982. The scheme is to add $Na_3Citrate$ to a boiling $AgNO_3$ solution. As shown by Turkevich in the case of gold, the reducing agent is also the nucleating agent which forms a mixed polymer of gold ions before the reduction takes place and upon reduction would turn into a small gold cluster. In the same manner in the case of silver, citrate anions reduce the Ag^+ cations into Ag atoms. Before the reduction of all the silver in the solution is complete the nucleation and growth are already started, this fact would cause a broad size distribution as can be seen in Fig. 3.3.

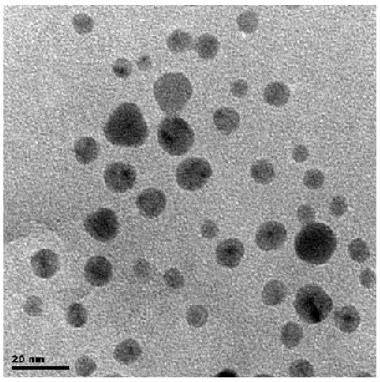

Figure 3.3: Typical size distribution of silver colloids in a regular Lee&Meisel type synthesis.

In our work an additional reagent, tannic acid, is used. Tannic acid as an additional nucleating agent that was used in the synthesis of gold MNPs by Slot and Geuze[38]. This reagent causes a rapid nucleation step separated in time from the growth process that will finally lead to a dispersion with a relatively good size distribution with a standard deviation of about 10%. A typical distribution of size and shape could be seen in Fig. 3.4

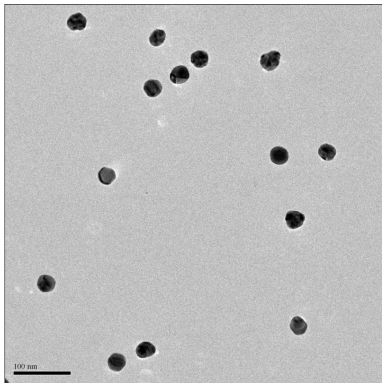

Figure 3.4: Typical size distribution of silver colloids in a our modified synthesis using tannic acid. To be compared with Fig. 3.3.

This size distribution could be further narrowed by purifying the dispersion in a gel electrophoresis apparatus. The particle dispersion is put inside a well of a high concentration agarose gel as could be seen in Fig. 3.5. The MNP mobility in the gel with an applied DC voltage depends on its diameter so the size distribution would "stretch" upon its movement in the gel . The gel is

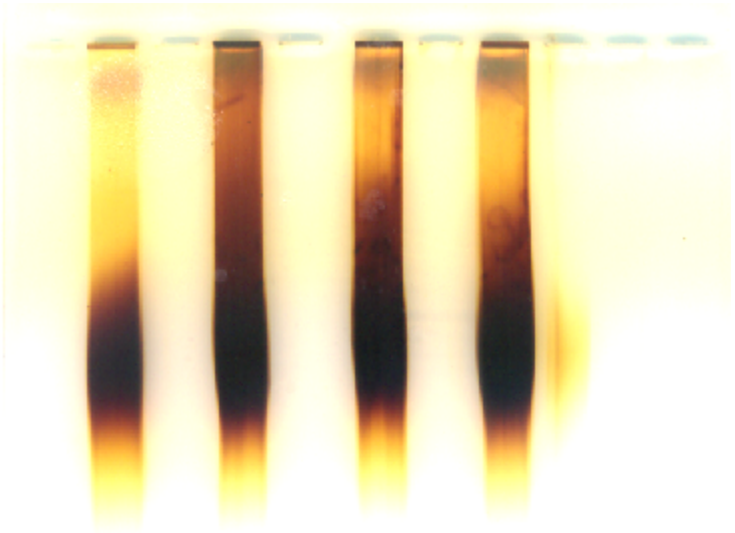

Figure 3.5: Narrowing the size distribution of MNP by gel electrophoresis. The size distribution of the particles "stretches" as it propagates through the gel. A fraction around the center of the distribution is cut from the gel and then extracted to a solution to give a narrower sized distribution of MNPs..

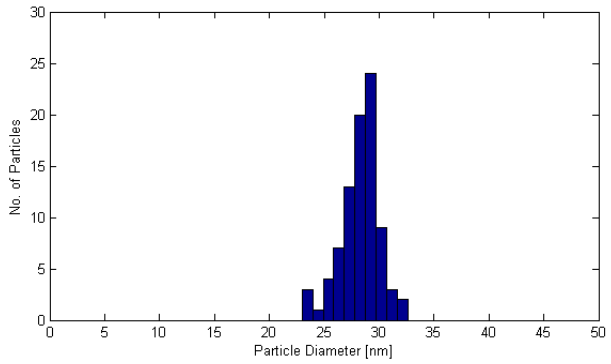

Figure 3.6: Diameter size distribution of a gel purified silver MNP dispersion.

cut around the center of the distribution and the particles are extracted from the gel. This process gave a size distribution with a standard deviation of 7% as could be seen in Fig. 3.6.

3.2.1.2 Silver MNP Stabilization.

Stabilizing the MNP dispersion against the formation of aggregates is crucial for making MNP conjugates. In our work we take advantage of two mechanisms in order to stabilize the particle dispersion against aggregation. The first is done by increasing the surface charge of the particles which causes an increased repulsion between the particles. In the synthesis process of the colloids I used citrate ions that have three acidic groups each carrying a negative unit charge and adsorb to the positively charged surfaces of the particles. This gives them an extra surface charge and raise the value of the repulsive potential. However, these charges are not permanently adsorbed on the surface. A more stable solution could be made by covalently binding negatively charged ligands by a thiol bond to the silver atoms at the surface of the particles. Thus, thiol ligands provide a more stable MNP in comparison with citrate ligands. The ligands I used have a negatively charged acid group(carboxyl), an organic molecule in the middle and an ending thiol (sulfur) group which covalently binds to silver. I used various thiolated ligands in order to stabilize the particles: MSA (mercapto-succinic acid), MUA(mercapto-undecanoic acid), MBA(mercapto-benzoic acid). Unfortunately this stabilization method is efficient only in electrolytic solutions with low ion concentration. However, all the methods I used for conjugation require high ionic concentration. The presence of a high concentration of ions in the solution causes screening of the repulsion of the particles which leads to aggregation. I had to search for an other stabilizing mechanism.

The second mechanism is thermodynamic. It incorporates the covalent binding of highly soluble long chain molecules to the surface of the particles. There are calculations [39] that show that dissolving these long chains in solution would raise the entropy of the system and it would be thermodynamically preferable over sticking the particles together by the Van Der Waals attraction. These molecules would also physically prevent the particles from reaching a very short distance were the Van Der Waals attraction is stronger.

The ultimate choice would be a ligand that incorporate the two stabilization mechanisms. I used thiolated PEG acid molecules. Like the other ligands it covalently binds to silver by the thiol group. The backbone of the molecule I used is a chain of 8 ethylene glycols. It is preferable over alkyl chains like the other ligands I used because it is highly soluble in water. In the end of

the chain there is a negatively charged acid group. Unlike the particles that were stabilized with the above ligands, the particles stabilized with this ligand have shown the ability to withstand strong centrifuging and high ionic strength biological buffers without showing aggregation. This stability gives the ability to concentrate the silver MNPs to unprecedented concentrations which is necessary for efficient conjugation. A silver MNP dispersion of a final concentration of $1\mu M$ was achieved after stabilizing the particles, which is 20,000 time more concentrated than the original, as prepared, dispersion.

3.2.2 The Preparation of MNP-QD Layered structures

The procedure in this work follows the work of Kottov [29]. The procedure consists of a few steps. The first step involves adsorbing PolyDialylDimethylAmmoniumChloride(PDADMAC), positively charged polymer on a clean glass microscope cover-slip. The polymer solution has to be of a sufficiently high ionic strength(0.5M NaCl) in order to prevent the polymers from stiffening and to also repel each other in the solution [30]. A thorough wash has to be applied to the surface to remove access polymer and to leave a mono-layer on the surface. The next layer is of negatively charged PolyStyreneSulfonate(PSS) with the same buffer solution(0.5M NaCl). This would again be followed by a thorough wash. The MNP or QD have both negatively charged surfaces, hence, their adsorption is done in the same manner. Since the interest is in single objects, aggregation of particles should be avoided, hence, the particles should preferably repel each other. That requires the solution to be of low ionic strength (no NaCl), such that there would be low screening of their repulsion.

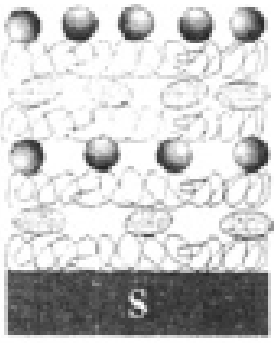

Figure 3.7: A scheme of a LBL MNP device [29].

In this work, devices with QD MNP layer separation of 7, 9, 13 and 19 poly-electrolyte layers were fabricated and measured. This method has a few drawbacks. First of all the objects are not ordered on the surface, hence the distribution of distances between a QD in the QD layer to a MNP in the MNP layer would be very broad. A possible solution to this would be to have a low density QD layer yet a high density MNP layer as was done in this work. But this has an additional disadvantage, a dense packing of the MNP would cause a shift to the plasmon frequency and increased scattering from the MNP surface that would make the measurement too noisy.

3.2.3 Preparation of MNP-QD conjugates

3.2.3.1 Preparation of MNP -QD Conjugates by LBL Coating of MNPs.

Conjugates are formed by first coating silver MNP with polyelectrolyte layers and then adsorbing QD on the top layer as was elaborated in the previous section. Unlike the wash steps in the process of film growth on a substrate, in this case the wash steps involve centrifuging of the dispersion. The coated massive MNP would travel to the bottom of the tube whereas the access lightweight polymer would remain in the bulk solution which is removed. A measure for altering the surface charge is obtained by running the sample in an electrophoresis apparatus. An agarose gel is made with wells inside. The particles are put in these wells and then a DC voltage is applied. The particles travel towards the negative lead since they are positively charged. This gives us and indication of polymer coating of the particles. There is another indication of polymer coating in

the TEM as a bright layer surrounding the silver particles. Conjugates are then formed by the reaction of a solution of CdSe/ZnS QD with a 1:1 ratio with polymer coated silver MNP.

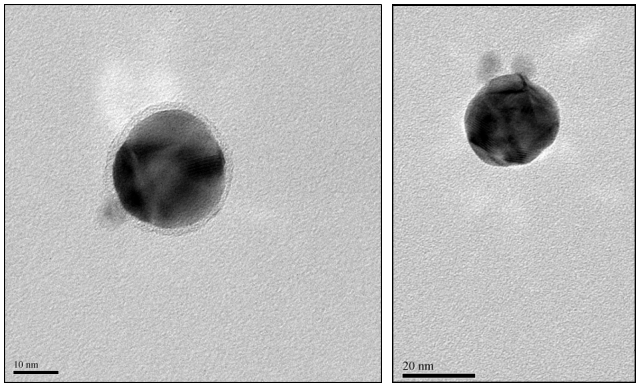

Figure 3.8: MNP-QD conjugates made by the layer by layer polymer coating method.

This methods adds complications to the assembly. It requires the use of centrifuging the solutions between each step of polymer adsorption in order to remove excess unbound polymer. It also requires the presence of high salt concentrations which is necessary both for preventing the polymer from stiffening and to avoid mutual repulsion of the polymers. These additions cause aggregation of particles and could be applied only on very stable MNP dispersions.

As could be seen in Fig. 3.8 this methods indeed resulted in MNP-QD conjugates but with only up to three layers of polymers due to a low yield after each stage of centrifuging. Another drawback is that conjugates with more than one QDs are formed in solution, hence this method of conjugation is not specific enough for single object measurement. This led us to choose an additional method of conjugation.

3.2.3.2 Preparation of MNP-QD conjugates using DNA

As discussed in section 2.3.3 a DNA single strand is covalently bound to a MNP and a complimentary DNA strand is bound to a QD. The MNP-QD conjugation is made by the specific attraction of DNA complementary single strands to form a double strand. The DNA serves as a spacer between the MNP and the QD. The double strand has a characteristic length of 0.3 nm per DNA base pair.

Binding DNA to MNPs. The method used by the Alivisatos group for binding the DNA to the MNPs relies on the replacement of phospine ligands on the MNP by the thiol group on the DNA oligo. This was found to be less suitable for silver MNPs. In my work instead of replacing the capping ligands of the MNP with a thiolated DNA I intend to link the end of the ligand, which has an ending carboxyl group, to an amino modified oligo DNA by using the method of EDC/NHS esterification. This way the particles would maintain their stability. The scheme of this reaction could be seen in Fig. 3.9.

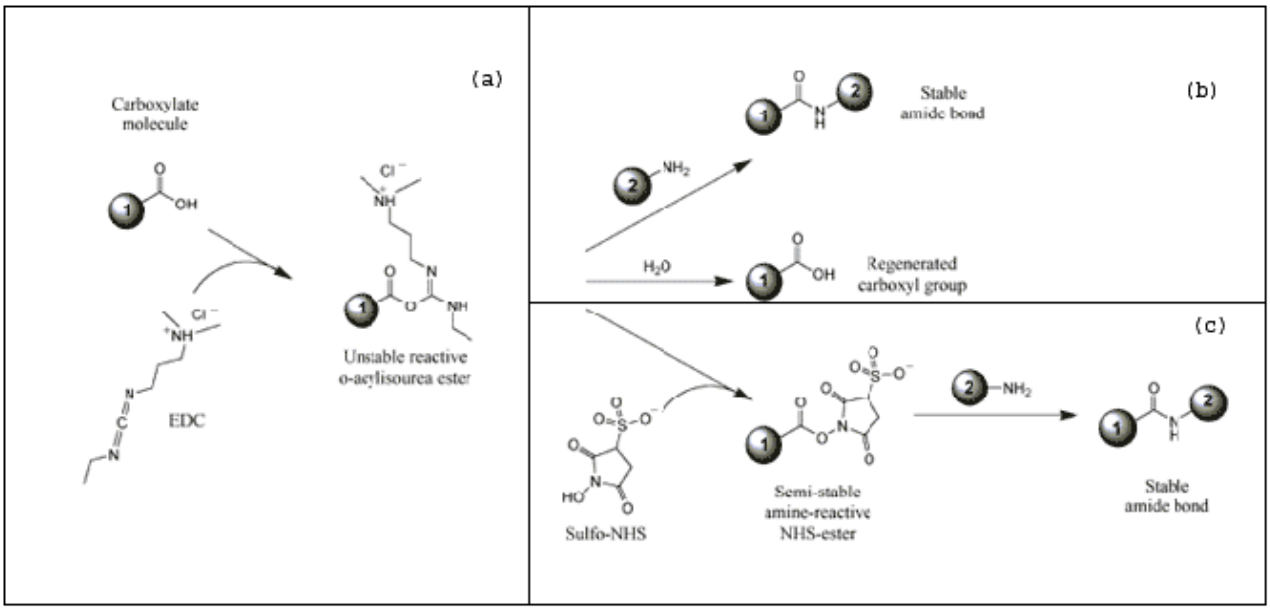

Figure 3.9: EDC/NHS cross-linking mechanism [Pierce Biotech]. (a) The reaction starts in the activation of the carboxyl group on the MNP (1) by the EDC molecule, turning it into an unstable active ester. (b) It is replaced by an amino-DNA (2) to form the desired MNP-DNA conjugate. The reaction is not efficient enough, the active ester is very short lived due to (b) hydrolysis. For improving this reaction another step is added. (c) A sulfo-NHS molecule replaces the EDC and the product is semi-stable NHS-ester which is then replaced by the amino-DNA (2) tail to form a stable amide bond. This can be used with any carboxyl ending ligand.

A single DNA strand on each and every MNP. Using the above synthesis method would result in MNPs with different number of strands on every particle. MNPs with different number

of DNA strands could be separated by gel electrophoresis. MNPs with more strands would move slower in the gel. This separation would be discreet because of the discreet number of the strands on the particles. The discreet separation of MNP-DNA conjugates relies on the ratio between the particle diameter and the DNA length. The lower this ratio is, the better the separation in gel electrophoresis would be. For having a good separation there is a need for a long enough DNA strand so that the ratio would be suitable for separation. However, the enhancement mechanism demands short separations between the MNP and the QD. I shall solve this problem by an initial separation step with a sufficiently long DNA and then I shall cut the DNA at a desired length.

Cutting the DNA. I put restriction sites in the DNA sequence after 15, 30 and 45 bases. These sites contain special palindromic sequences that could be identified by specific restriction enzymes. These enzymes find the restriction sites and cut the DNA exactly at that specific site. After the separation of the MNP-DNA conjugates into discrete bands I would select the band I want for conjugation. After that I shall apply the appropriate restriction enzyme and have MNP-DNA single conjugate. applying this process for both MNPs and QDs give the ability of creating conjugates with a well defined separation.

DNA conjugate verification. The method I use for verifying DNA binding to the MNPs uses radio-labeling of the DNA. The DNA is extended by another base which has a beta emitting isotope ^{32}P. Running the products in an electrophoresis apparatus separates unbound DNA and MNP-DNA conjugates. A photographic film is exposed to the gel and give an indication to the conjugation. A conjugation is evident if there is an overlap between the visibly seen MNP band and the exposed film showing a band of labeled DNA. Fig. 3.10 shows a characteristic verification process.

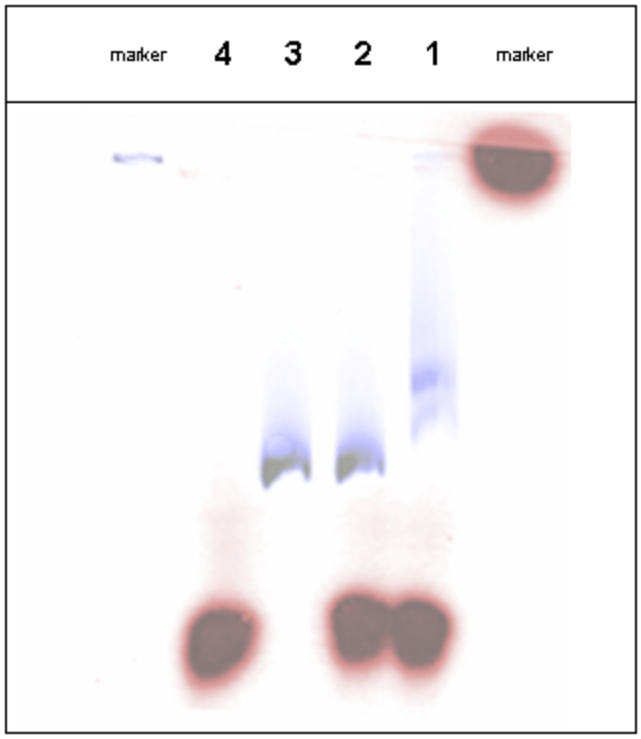

Figure 3.10: Conjugate verification. A film exposed to a gel with QD DNA reaction mixture (red) is superimposed on a UV absorption image (blue) of that gel. *1.* Reaction mixture of QDs, linker molecules, and amino-modified DNA. *2.* A control consisting of QD and DNA with no linker molecule. *3.* A second control of bare QD solution. *4.* A third control of bare DNA solution. The reaction mixture *1.* shows aggregation of QDs that is evident in the discreet band of dimers and higher order aggregates .

3.3 Fluorescence Measurements

3.3.1 Fluorescence Measurement of Single Submicron Objects.

3.3.1.1 Measurements of Integrated Intensities.

I used the LSM 510 laser scanning microscope. The measurements in this setup are based on cutting the high frequency blue light of the laser by a low pass filter that allows the transmission

of redshifted fluorescence. The measurement is done on a sample of MNP and QD layers with a number of polyelectrolyte layers separation. The sample is excited by a laser in resonance with the MNP plasmon. The intensity of the coupled MNP-QD emission is recorded and should be compared to the emission intensity of bare QDs. This kind of measurement was done for different MNP QD separations.

Data analysis. Images are analyzed with a graphics software (ImageJ) that has the ability to identify objects in pictures. Spots which are diffraction limit in size are chosen and their location is recorded.

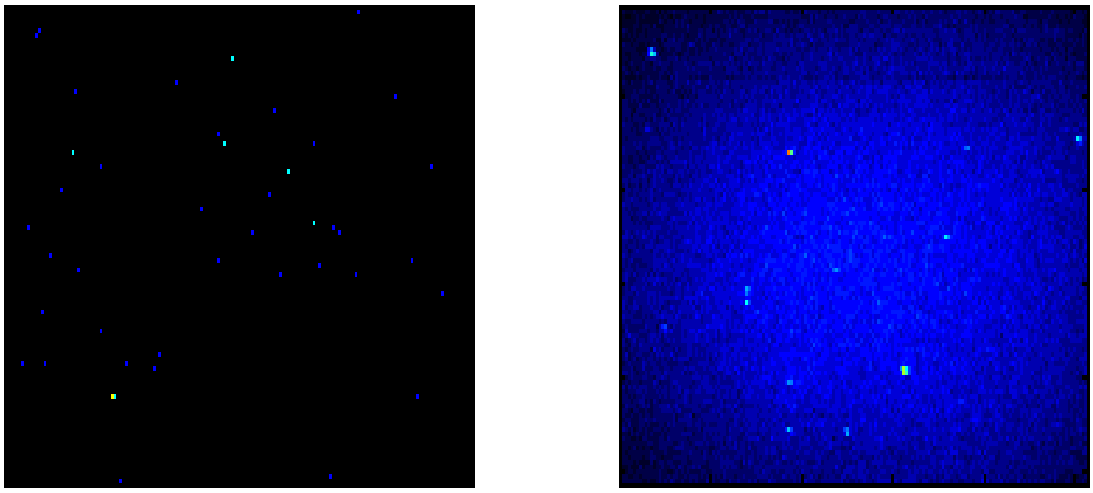

Figure 3.11: Bare QD emission (left) and MNP coupled QD emission (right).

The intensities should be normalized to the intensity of the background scattering. The scattering was found to be inhomogeneous throughout the surface for the following reason. In the laser scanning microscope, the scan is done by scanning the laser beam in proximity to the focal axis of the objective this means that the illumination intensity would be lower when not aligned exactly with the focal axis. This is observable when there is large scattering from the surface like in the case of the silver MNP covered samples.

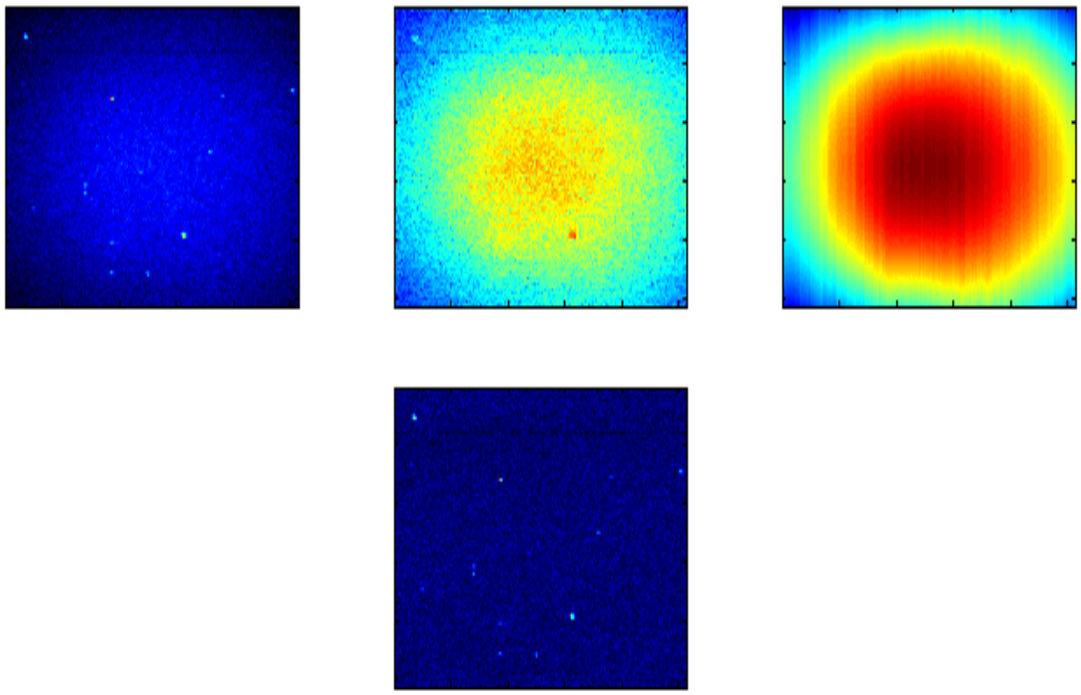

Figure 3.12: Normalizing the emission intensity by a polynomial fit.

The emission would be normalized to the background scattering with a value given by a fit to a polynomial function. The images are then divided by that background function and give the normalized intensity of the QD emission. The intensity of each spot is summed over a box of radius 5X5 pixels which correspond to a box of 350X350 nm and give the intensity of the QD in this band.

This intensity is unitless, it gives a measure of how well above the background is the measured QD intensity. The same process is done both to the region of bare QD and for images from the coupled QD MNP emission. In order to get the enhancement factor the whole distribution has to be multiplied by the ratio of the average background of the images. This would set them on the same scale for comparison. An example is given for the distribution of intensities for a MNP QD separation of 13 layers (6.5 nm average separation) in Fig. 3.13

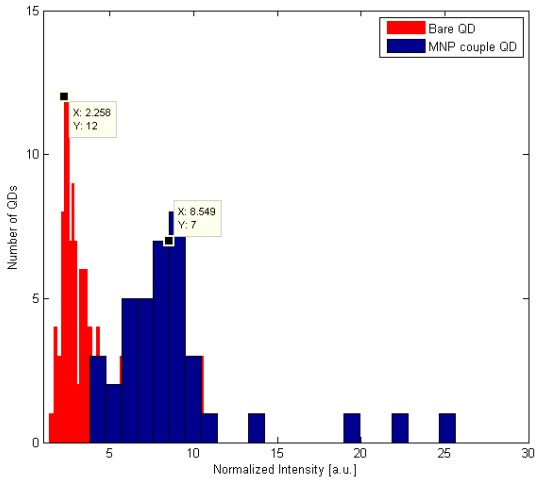

Figure 3.13: Bare QD emission (red) and MNP coupled QD emission (blue).

This measurement show an average enhancement of the emission intensity by a factor of 3.5 with a tail of as much as 10 fold enhancement. Due to the large scattering of the background I suspect these measurements. A low pass filter has a limited efficiency and is not good enough in cutting intense scattering like in the case of silver MNP layers. This understanding lead me to try to characterize the emission by its spectrum. Having spectral separation with a grating would diminish the background scattering with much better efficiency.

3.3.1.2 Measurements With Spectral Data

The following measurement was done on a LSM5-Meta in lambda mode. This is a laser scanning confocal microscope which has an argon lase at 458nm. Emitted light collected by the objective is separated in to channels by their wavelength with 10nm resolution, where each channel is amplified by a photomultiplier tube. Each channel gives an image of the intensity of fluorescence in that band. A typical set of images can be seen in Fig. 3.14.

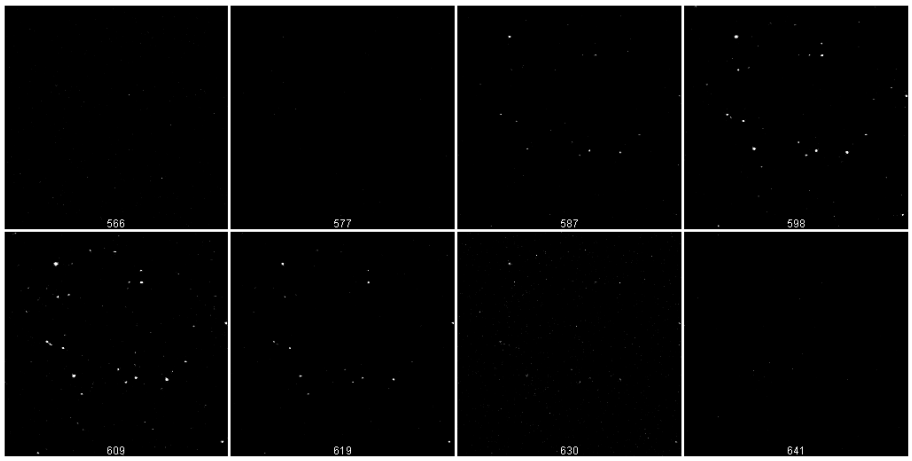

Figure 3.14: Confocal Microscope image of QDs emission divided into channels of 10 nm width. A peak of the intensity is evident around 600 nm.

The emission spectrum of each dot is obtained and the sum of intensities in the peak of 600nm is the QD emission intensity. This process gives the distribution of the QD emission intensities which is to be compared with the distribution of intensities of the enhanced QDs. The results of such a measurement are shown in Fig. 3.15.

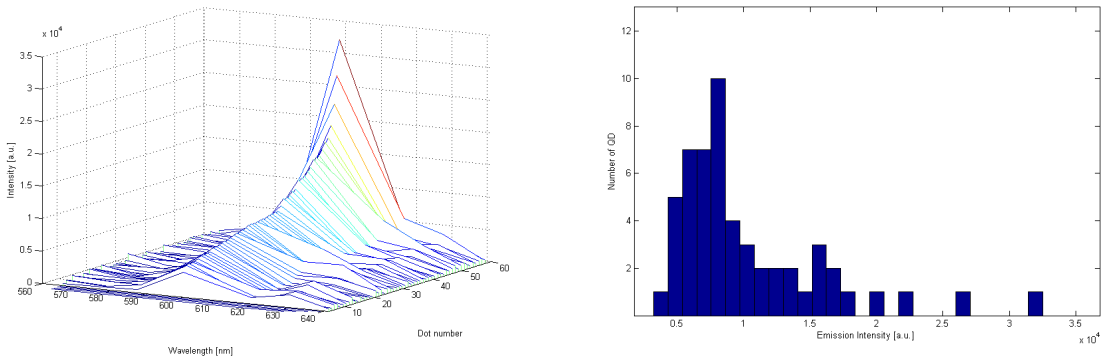

Figure 3.15: QD emission spectra (left) and intensity distribution (right) of Fig. 3.14.

This data has to be compared with the intensity of the QD emission coupled to silver MNP. Unfortunately the dense silver MNP film gave too much scattering and the emission enhancement of the QDs could not be verified. The problem of intense scattering from dense MNP films raises

a question mark around this kind of measurements. A more detailed study should be conducted on single MNP-QD conjugates.

3.3.2 Fluorescence Measurement of MNP-QD Conjugates.

The fluorescence measurement in solution was done on a Jobin Yvon Flurolog3 fluorimeter. A typical setup could be seen in appendix A. An excitation wavelength of 402 nm, in resonance with 30 nm silver MNPs, was selected by the excitation monochromator. Emission was collected after passing the emission monochromator. Both excitation and emission slits were of 5 nm bandwidth.

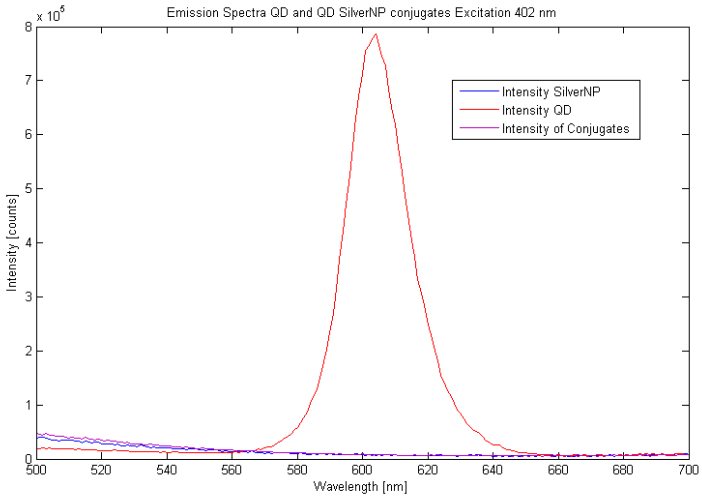

Figure 3.16: Quenching of fluorescence of QD by silver MNPs.

The measurement of a solution of silver MNP QD conjugates with one and three polymer layers separation resulted in quenching of the fluorescence by at least a factor of 40. It was below the value obtained by the scattering tail of the silver MNP in the emission wavelength of the QD. The reason for the total quenching is because of the advantage of non radiative energy transfer from the QD to the MNP over the absorption enhancement mechanism in these short distances. The reason for that is the disability of this method to yield a decent separation between the MNP and the QD.

Chapter 4

Conclusions

Fluorescence measurements of MNP-QD coupled layers were done using a low pass filter gave an enhancement of fluorescence (section 3.3.1.1). The distribution of intensities was enhanced by a factor of 3.5 for a device with MNP QD separation of 13 polymer layers (about 7 nm). Due to large scattering from the silver MNPs there is still a doubt about the these measurements. Measurements with spectral capability gave us the certainty in the measurement of fluorescence from bare QDs which showed their regular emission at 600 nm. But in the case of MNP-QD coupled layers, the emission intensity was comparable to the background scattering and could not be distinguished. Because of this problem the measurements are inconclusive.

The current results show the necessity of creating single MNP-QE conjugates with a well defined separation. As a first step, an ensemble measurement of fluorescence of MNP-QD conjugates was conducted in an aqueous solution. The fluorescence of solution of MNP-QD conjugates with a separation of 1 and 3 layers of polymer layers (about 0.5-1.5 nm) were quenched by at least a factor of 40 comparing to a bare QDs solution. This is understood by the mechanism of non radiative energy transfer from the QD to the MNP. The creation of MNP-QD conjugates with a larger separation gave a low yield, with a concentration below the detection limit of solution measurements. Preliminary work was conducted on making single MNP-QD conjugates by DNA cross-linking which allow specific conjugation with a well defined separation.

In this work I have shown a novel way of mass measurements characterizing the intensity of

fluorescence of single emitting objects. I have shown a promising way of synthesis of silver MNPs with a narrow size distribution. These MNPs dispersions are extremely stable and their surface could be modified for cross-linking. I have the capability of creating monolayers of MNPs and QDs with a varying density that could be used for measurements and for fabrication. Having single MNP-QD conjugates would make the characterization of the enhancement possible and will open a way for new experiments and applications.

Chapter 5

Appendix

Appendix A - Fluorescence Measurements Setups.

Fluorescence Measurements In a Solution

A typical apparatus for measuring fluorescence of a bulk liquid specimen could be seen in Fig. 5.1.

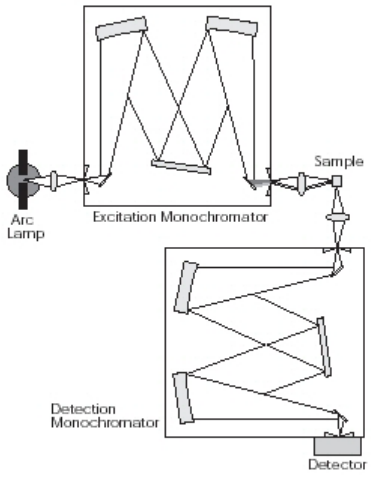

Figure 5.1: A fluorimeter apparatus [SpectralProducts].

The sample is put inside a cuvette, a transparent quartz tube. White light from an arc lamp enters the excitation monochromator and only a narrow band of frequencies is illuminated on the

sample. Emitted light from the sample is collected at 90 degrees and is focused on the detection monochromator entrance slit. The light is detected by a PMT detector. This apparatus gives the ability to measure the emission spectrum of a sample as well as the excitation spectrum of the sample. This kind of measurements give the total value of the emission from the whole liquid sample and does not have the capability to detect single objects. This is the reason for using other systems as well.

Fluorescence Measurements of Single Submicron Objects - The Confocal Laser Scanning Microscope

For measuring fluorescence from single objects smaller than diffraction limit, there is a need to concentrate light and make samples with average density smaller than the inverse the diffraction limit spot radius cubed. This could be done by adsorbing dilute samples on transparent slides and using an apparatus with diffraction limit resolution. A realization of such a system is the epifluorescence microscope as can be seen in Fig. 5.2.

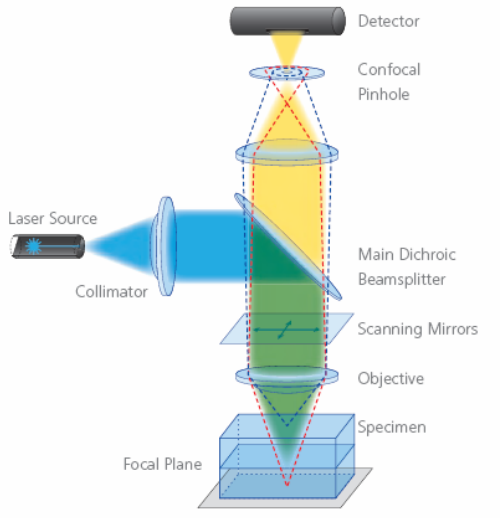

Figure 5.2: A confocal microscope setup [Zeiss].

Laser light coming from the left is collimated and reflected in 90 degrees by the dichroic beamsplitter. The light is then focused by the objective lens to a diffraction limit spot on the specimen.

The emitted as well as the reflected light is collected by the same objective and is collimated and reaches again the dichroic beam-splitter. The red shifted emitted light from the specimen goes through the dichroic beam-splitter and focused on the detector. The reflected laser light is cut and reflected the second time, and does not go through to the detector. The confocal pinhole gives a better z axis resolution as light of different colors having different focal length would be cut by the pinhole as can be seen in Fig. 5.2.

In this work I used Laser Scanning confocal microscope that together with the confocal setup, has ultra fast scanning mirrors that enable fast scans of the specimen surface by moving the laser beam. This feature allows the collection of large amounts of data in short times. Another extension of this microscopy system is called spectral imaging. Instead of having a single detector to collect all the emitted light, the light is first dispersed by a grating and divided into channels with a spectral resolution of 10 nm. This allows not just the identification of diffraction limit spot objects but also gives full spectral data from each point.

Appendix B- Experimental Protocols

Silver MNP synthesis

The procedure used in this work is a modified Lee and Meisel procedure. Silver Nitrate solution is heated to 95^0C. A heated solution of tri-sodium citrate and tannic acid is added. The solution immediately changes color and turns yellowish which is the result of absorbance of the blue light by the silver particles. The solution is heated on a hot plate in 95^0C for 20 min. A dispersion of 30 MNP would be used in the case of making MNP QD conjugates. This silver MNP solution was named ETA16. After 8X dilution it had an absorbance maximum at $\lambda = 400$nm with a value of Abs=0.541. A calculation of the extinction coefficient for the measured 28.5±10% nm mean diameter a value of $1 \cdot 10^{10} M^{-1} cm^{-1}$ under the assumption that all the silver in the reaction turned into silver particles.

A dispersion of 60 nm MNP is used in the case of the thin films experiment. Their plasmon resonance is in $\lambda = 458$ nm which is exactly like one of the lines of the Argon laser available in the

case of measuring thin films on the Zeiss laser scanning microscope.

Dispersion Concentration and Stabilization

In order to have a high yield of conjugates, an extremely high concentration of silver MNP is required. This could only be achieved with a very stable dispersion because centrifuging the dispersion exerts very strong forces on the particles which lead to aggregation of the particles. 1 liter of as prepared cooled particle solution was then concentrated to a volume of 80 ml in a SLA 3000 rotor in a Sorval centrifuge for 30 minutes at 10,800 RCF at 4^0C. Defrost thiol-dpeg^{8}acid 1.5 mM was used as the stabilizing ligand. It has eight units of polyethylene glycol with a carboxylate group at one end and a thiol group at the other hand. It was added in a 10 fold dilution and left for at least 20 min of reaction. The solution was again concentrated with a small Sorval rotor to 5.5 ml and then to 200 μl with a table top centrifuge of Eppendorf tubes at 10,800 RCF. A small fraction of the final concentrated solution was taken and diluted x20,000 and absorbance measurement of 0.456 at λ_{max}= 401 nm yielded a final concentration of 0.93μM.

LBL Device Fabrication

The device for this experiment were produced with the LBL coating of surfaces method. The samples consist of 3 layers of poly-electrolytes (glass + - +) these layers would give a homogenized layer of positively charged surface. After that adsorption of 1 nM solution of QD that carry negative surface charge was applied for 10 min. On top of that an additional negative layer was adsorbed in order to complete a negatively charged layer. On top of that 7/9/13/19 layers were adsorbed, ending with a positive layer. The width of each layer is said to be of about 0.5 nm. The last layer is of negatively charged ETA7 60nm MSA (Mercapto-Succinic Acid, Sigma) coated silver MNP of a concentration of $4 \cdot 10^{-11}$M kept at pH 9 (adjusted with NaOH). These MNP had a plasmon resonance at 458 nm, which exactly coincide with a line of an Argon laser available in the Zeiss LSM 510 and the LSM5-META confocal microscope. The last layer of silver MNPs was adsorbed by half dipping the sample into the particle solution inside a cover-slip box overnight. This way both a control and a measurement is being done on the same sample.

LBL Coating of Silver MNPs.

Concentrated 30 nm stock silver MNP solution was diluted 500X in DDW (doubly distilled water). 50 μl of the particle solution was mixed with 50μl 2mM NaCl. To this solution, 10 μl of 10 mg/ml PDADMAC(MW<100,000 Sigma) in 1mM NaCl was added and left to stand for 20 minutes. DDW was added to a volume of 1000 μ l and was centrifuged for 10 min at 10,000 RPM. 980 μl was of clear solution was removed from the top and 20 μ l of dark solution remained at the bottom of the tube. This washing process was done a second time and 25 μ l were left. 12.5 μl was diluted x800 and measured absorbance of 0.256 at 402nm which corresponds to 1.96 nM concentration of coated particles before the dilution. No shift of the plasmon resonance was observed.

Bibliography

[1] M. Faraday, Philos. Trans. R. Soc. London 1857, 147, 145.

[2] L. Tonks: Phys. Rev. 38, 1219 (1931).

[3] S. A. Maier and H. A. Atwater, "Plasmonics: localization and guiding of electromagnetic energy in metal/dielectric structures," J. Appl. Phys. 98, 011101 (2005).

[4] W.L. Barnes, A. Dereux, and T.W. Ebbesen, Nature (London) 424, 824 (2003)

[5] Sonnichsen, C.; Reinhard, B. M.; Liphardt, J.; Alivisatos, A. P. Nat. Biotechnol. 2005, 23, 741-745.

[6] A.M. Glass, P.F. Liao, J. G. Bergman, and D.H. Olson, Opt. Lett. 5, 368 (1980).

[7] K. T. Shimizu, W. K. Woo, B. R. Fisher, H. J. Eisler, and M. G. Bawendi, Phys. Rev. Lett. 89, 117401 (2002).

[8] J. Gersten and A. Nitzan, J. Chem. Phys. 75, 1139 (1981).

[9] Jian Zhang, Yi Fu, Mustafa H. Chowdhury, and Joseph R. Lakowicz, Nano Letters, 2007 7, 7, 2101-2107.

[10] Olga Kulakovich, Natalya Strekal, Alexandr Yaroshevich, Sergey Maskevich, Sergey Gaponenko, Igor Nabiev, Ulrike Woggon, and Mikhail Artemyev, Nano Letters 2002 2, 12, 1449-1452.

[11] Robert I. Nooney, Ondrej Stranik, Colette McDonagh, and Brian D. MacCraith, Langmuir 2008, 24, 11261-11267.

[12] H. Mertens, A. F. Koenderink, and A. Polman, Phys. Rev. B 76, 115123 (2007).

[13] Jean-Michel G´erard and Bruno Gayral JOURNAL OF LIGHTWAVE TECHNOLOGY, 17, 11, 2089 (1999).

[14] Govorov, A. O.; Bryant, G. W.; Zhang, W.; Skeini, T.; Lee, J.; Kotov, N. A.; Slocik, J. M.; Naik, R. R. Exciton-plasmon interaction and hybrid excitons in semiconductor-metal nanoparticle assemblies. Nano Lett. 2006, 6 (5)), 984–994.

[15] G. Mie, Ann. Phys. 25, 377 1908.

[16] J. A. Stratton , Electromagnetic Theory, McGraw-Hill Book Company (1941).

[17] M. Born, E. Wolf, Principles of Optics.

[18] U. Kreibig and M. Vollmer, Optical Properties of Metal Clusters Springer, Berlin, 1995.

[19] Maier, Stefan A. Plasmonics: Fundamentals and Applications, 2007.

[20] Seogjoo Jang, J. Chem. Phys. 127, 174710 (2007)

[21] David Pines, Elementary Excitaions In Solids, 1963.

[22] U. Kreibig , Z. Physik 234, 307- 318 (1970).

[23] E.A. Hauser, J. E. Lynn, Experiments in Colloid Chemistry, McGraw Hill, New York, 1940.

[24] J. Turkevich, P.C. Discuss. Faraday Soc. 1951, 11, 55.

[25] R Zsigmondy, Z. Phys. Chemie 1906, 56, 65.

[26] B.W. Ninham, Advances in Colloid and Interface Science, 83, 1-17 (1999).

[27] F. Caruso, Colloids and Colloid Assemblies, Wiley-VCH, 2004.

[29] Nicholas A. Kotov, Imre DCkiiny, and Janos H. Fendler, J. Phys. Chem. 1995, 99, 13065-13069.

[30] David I. Gittins and Frank Caruso, J. Phys. Chem. B 2001, 105, 6846-6852.

[31] Langmuir, Irving, U. S. Patent 2,232,539 (General Electric Co.) February 18, 1941.

[32] G. Decher, Science, 277, 29 (1997).

[33] F. Caruso, H. Lichtenfeld, M. Giersig, and H. Mohwald, J. Am. Chem. Soc. 1998, 120, 8523-8524.

[34] Shelley A. Claridge, Huiyang W. Liang, S. Roger Basu, Jean M. J. Fréchet, and A. Paul Alivisatos, Nano Letters, 2008 8, 4, 1202-1206.

[35] D. Zanchet, C. M. Micheel, W. J. Parak, D. Gerion, S. C. Williams, and A. P. Alivisatos, J. Phys. Chem. B 2002, 106, 11758-11763.

[36] J. Yguerabide and E. E. Yguerabide, Anal. Biochem. 262, 137–156 (1998).

[37] P. C. Lee and D. Meisel, J. Phys. Chem. 1982, 86, 3391-3395.

[38] J. W. Slot and H. J. Geuze, Eur. J. Cell Biol. 38, 87, (1985).

[39] Samuel A. Safran, Statistical Thermodynamics of Surfaces, Interfaces, and Membranes.